Journal of
Marine Science and Engineering

MDPI

Article

Remote Sensing of the Coastline Variation of the Guangdong–Hongkong–Macao Greater Bay Area in the Past Four Decades

Ruirui Hu [1,2,†], Lijun Yao [3,†], Jing Yu [2,*], Pimao Chen [2] and Dongliang Wang [2]

1 College of Marine Science, Shanghai Ocean University, Shanghai 201306, China; m190200515@st.shou.edu.cn
2 South China Sea Fisheries Research Institute, Chinese Academy of Fishery Sciences, Scientific Observing and Experimental Station of South China Sea Fishery Resources and Environment, Ministry of Agriculture and Rural Affairs, Key Laboratory of Marine Ranching Technology, CAFS, Guangzhou 510300, China; chenpm@scsfri.ac.cn (P.C.); 13067438786@163.com (D.W.)
3 Department of Optoelectronic Engineering, Jinan University, Guangzhou 510632, China; tylj@jnu.edu.cn
* Correspondence: yujing@scsfri.ac.cn
† Ruirui Hu and Lijun Yao contributed equally to this work.

Abstract: In this study, a combination of example-based feature extraction and visual interpretation was applied to analyze the coastline variations in the Guangdong–Hong Kong–Macao Greater Bay Area (GHMGBA) from the past four decades based on the Landsat satellite remote sensing image data from 1987–2018, using ENVI and ArcGIS software. The results showed that the total length of the coastline of the GHMGBA increased in the past four decades, rising from 1291 km in 1987 to 1411 km in 2018. Among these, artificial coastline increased by 450 km, while the other coastline types decreased. The type of coastline that decreased the most was bedrock coastline, by a total of 172 km. The silty coastline disappeared, and almost all of it was converted to artificial coastline. Variations in the coastline of the GHMGBA were mainly connected to human activities and showed an overall trend of advancing towards the ocean. Dynamic monitoring of coastline variations can provide a reference for the protection of natural resources, sustainable marine development and rational planning of the coastal zone.

Keywords: Landsat; feature extraction; visual interpretation; ENVI; ArcGIS; Guangdong–Hong Kong–Macao Greater Bay Area

check for updates

Citation: Hu, R.; Yao, L.; Yu, J.; Chen, P.; Wang, D. Remote Sensing of the Coastline Variation of the Guangdong–Hongkong–Macao Greater Bay Area in the Past Four Decades. *J. Mar. Sci. Eng.* **2021**, *9*, 1318. https://doi.org/10.3390/jmse9121318

Academic Editor: Gerben Ruessink

Received: 16 October 2021
Accepted: 15 November 2021
Published: 23 November 2021

Publisher's Note: MDPI stays neutral with regard to jurisdictional claims in published maps and institutional affiliations.

Copyright: © 2021 by the authors. Licensee MDPI, Basel, Switzerland. This article is an open access article distributed under the terms and conditions of the Creative Commons Attribution (CC BY) license (https://creativecommons.org/licenses/by/4.0/).

1. Introduction

A coastline is the boundary line between land and sea, located in the sensitive transition zone extending from both regions [1] and refers to the boundary reached by high tide [2]. It is an area where human activities are more concentrated and resources and environmental conflicts are the most prominent [3]. The changes on coastlines are the result of the interaction between human activities and natural factors, reflecting the mutual influence among economy, society and ecology. The study of coastline variation plays an important role in the natural resources and ecological protection of the coastal zone. Studies have shown that the major reasons for the coastline changes in the Pearl River Estuary (PRE) were government policies, regulation of the estuary, urban construction and beach reclamation [4–8].

The areas with the greatest changes were the Nansha District of Guangzhou and the Nanshan District of Shenzhen [9]. Scholars in the field conducted research on the eight estuaries of the PRE [5,10], both sides of Lingdingyang [11], the PRE region [4,6] and other small areas. For a larger area, such as the Guangdong–Hong Kong–Macao Greater Bay Area (GHMGBA), which includes the PRE, the coastline variability at a longer time scale (nearly four decades) remains unclear.

Traditional coastline survey means are not effective in measuring extensive areas or those with large topographic relief, complex coastlines. In addition, it can be challenging to study long-term changes using this method only [12]. Satellite remote sensing has the advantages of wide observation coverage, long time, convenient data acquisition and small restricted range [13–15]. It has been successfully applied to studies that have looked into coastline variation [16–18], sedimentation area change [19], reclamation monitoring [20,21], beach area change [22–24], aquaculture area change [25,26], land use change [27] and vegetation cover change [28].

Currently, automatic extraction and visual interpretation are two major coastline extraction methods that are widely used by researchers in this field of study. The automatic extraction method is another means to identify the coastline relies, and it relies on the differences in spectral features exhibited by different land use types on remote sensing images [29]. Commonly used methods include the edge detection algorithms [30] (Sobel, Canny, Roberts and other classical operators [31]), object-oriented method [32], region growing method [33–35], mathematical morphology method [36]) and threshold segmentation method [37].

However, the automatic extraction of coastline has issues with "same spectrum and heterogeneity" (same spectrum but unique features), inaccurate location due to the influence of mixed pixels and low accuracy of silty coastline extraction [38]. On the other hand, the visual interpretation method can be to recognize remote sensing images according to the interpretation marks.

The GHMGBA is a city cluster comprising two special administrative regions, Hong Kong and Macau and nine cities in Guangdong Province, i.e., Guangzhou, Shenzhen, Zhuhai, Foshan, Zhongshan, Dongguan, Huizhou, Jiangmen and Zhaoqing. It is an important area for China to build a world-class city cluster and take part in the competitive global scenario [39]. The region is also the most economically active region and an important growth pole in China at present [40]. It is the fourth largest bay area in the world after New York Bay Area, the San Francisco Bay Area in the United States and the Tokyo Bay Area in Japan, with a superior geographical position and diverse coastline types [4,41].

Since China's reform and opening up in the 1980s, these coastal cities have developed rapidly, especially in the areas where human activities are frequent. As a new world-class city cluster, the GHMGBA is a demonstration area for in-deep cooperation between the mainland, Hong Kong and Macao and also a positive reinforcement for implementing the "One Belt, One Road" initiative [42].

Computer graphics image processing technology and extraction software support automatic coastline monitoring [29]. Satellite remote sensing provides different periods of information of the coastline, reducing the engineering investment of manual measurement and shorting the repair and measurement cycle [14]. Studying the long-term evolution of coastline is of great significance for ecological environment protection and scientific management of the coastal zone [43]. The dynamic monitoring of coastline variations could provide a reference for the protection of natural resources, sustainable marine development and rational planning of the GHMGBA coastal zone.

2. Materials and Methods

2.1. Study Area

The study area is located in the northern South China Sea (SCS), 112.3°–115.05° E, 21.6°–22.85° N, including the coastal areas of Hong Kong, Macao, Guangzhou, Shenzhen, Zhuhai, Zhongshan, Dongguan, Huizhou and Jiangmen (Figure 1).

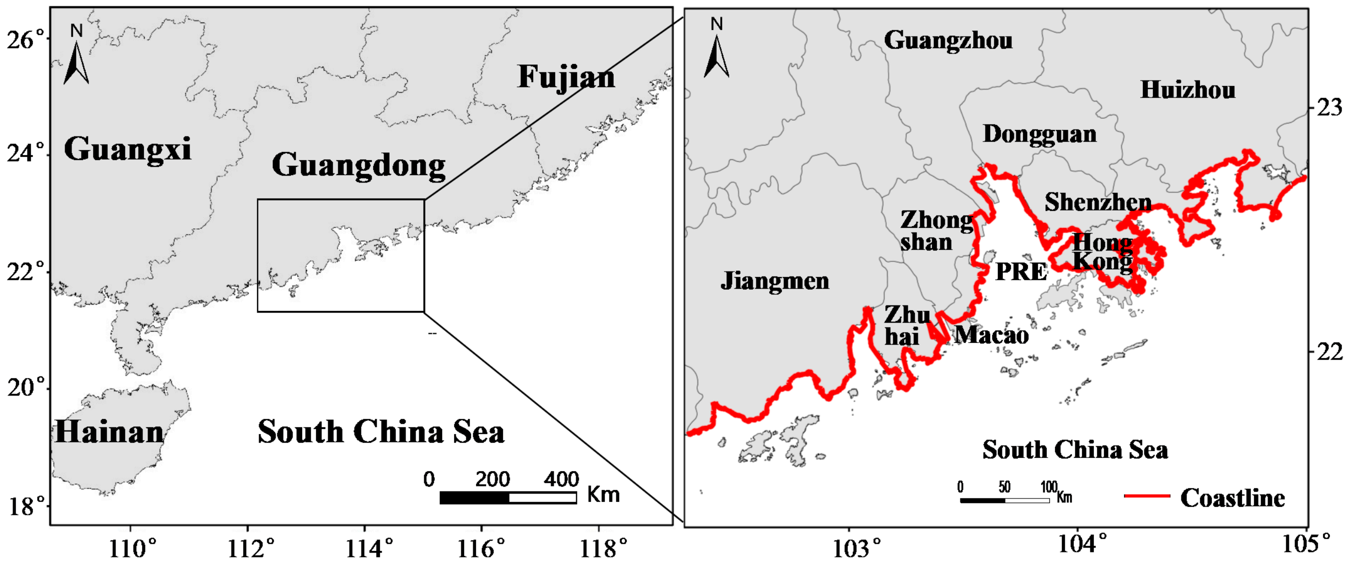

Figure 1. Study area.

2.2. Data Sources

The Landsat satellites are oceanic land resource satellites launched by NASA and are a type of technology that enables effective multi-temporal dynamic monitoring of coastlines. In this study, Landsat images for nearly 4 decades from 1987 to 2018 were obtained (http://www.gscloud.cn/, accessed on 10 May 2020), including 10 Landsat-5 TM images in 1987 and 1990, 10 Landsat-7 ETM images in 2000 and 2010 and five Landsat-8 OLI images in 2018 (Table 1). Among them, 1987–1990 represents the 1980s, 1990–2000 represents the 1990s, 2000–2010 represents the 2000s, and 2010–2018 represents the 2010s.

Table 1. Remote sensing data.

Date (dd/mm/yy)	Satellite	Sensor	Resolution	Orbit
09/03/2018	Landsat-8	OLI	30 m	121-44
03/10/2018	Landsat-8	OLI	30 m	121-45
01/04/2018	Landsat-8	OLI	30 m	122-44
03/05/2018	Landsat-8	OLI	30 m	122-45
23/03/2018	Landsat-8	OLI	30 m	123-45
08/10/2010	Landsat-7	ETM	30 m	121-44
08/12/2010	Landsat-7	ETM	30 m	121-45
28/10/2010	Landsat-7	ETM	30 m	122-44
28/10/2010	Landsat-7	ETM	30 m	122-45
20/11/2010	Landsat-7	ETM	30 m	123-45
16/04/2000	Landsat-7	ETM	30 m	121-44
15/09/2000	Landsat-7	ETM	30 m	121-45
01/11/2000	Landsat-7	ETM	30 m	122-44
01/11/2000	Landsat-7	ETM	30 m	122-45
20/08/2000	Landsat-7	ETM	30 m	123-45
22/10/1990	Landsat-5	TM	30 m	121-44
22/08/1991	Landsat-5	TM	30 m	121-45
14/09/1991	Landsat-5	TM	30 m	122-44
14/09/1991	Landsat-5	TM	30 m	122-45
02/09/1990	Landsat-5	TM	30 m	123-45
19/12/1988	Landsat-5	TM	30 m	121-44
03/12/1988	Landsat-5	TM	30 m	121-45
08/12/1987	Landsat-5	TM	30 m	122-44
08/12/1987	Landsat-5	TM	30 m	122-45
10/09/1987	Landsat-5	TM	30 m	123-45

The resolution of data was 30 m. In order to ensure the successful extraction of coastline data, all the remote sensing images were obtained from images with cloud cover less than 10% and images with unobstructed coastline. The quality of the collected data fully meets the requirements of this study. We obtained the vector maps (2017) of the GHMGBA with 1:1 million geographic data (https://www.webmap.cn, accessed on 22 May 2020) that could be tested based on coastline extraction accuracy. The PRE is a weak-tide estuary, and the tide does not have a significant impact on the long-term variation of the coastline [5]; therefore, it is not considered in this study.

2.3. Coastline Extraction and Classification

In this study, a combination of example-based feature extraction [44,45] and visual interpretation [46] was used to extract coastline data. Using ENVI 5.3.1 (Exelis VIS, Silicon Valley, CO, USA) software, the acquired Landsat images were preprocessed hrough a series of procedures, including image mosaicking, registration, clipping and stripe repair. The object-oriented feature extraction method based on samples was applied to segment the preprocessed image. According to the interpretation signs and the principles of extraction, the features of the study area were then segmented and merged into two categories: marine and land, and the boundary between them was the coastline.

During this process, vector data of the coastline were obtained. Using ArcGIS 10.3 (Esri, Redlands, CA, USA) software, false color band combination and appropriate image enhancement processing were applied to Landsat images to improve the distinguishability of coastline. The coastlines of the study area were classified into five types: artificial, bedrock, biological, sandy and silty coastlines [47–49] (Figure 2). Based on the established coastline interpretation signs and principles of extraction, the visual interpretation method was adopted to classify the automatically extracted boundary and correct the coastline (Figure 3).

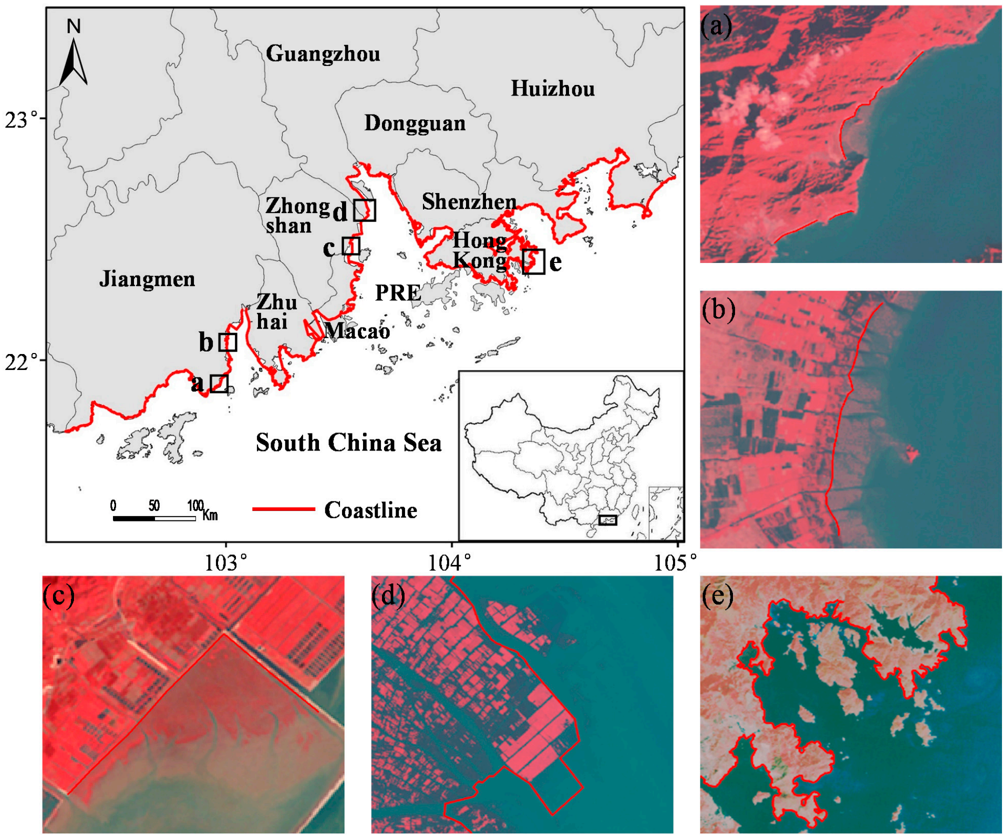

Figure 2. Map of interpretation marks of the coastline: (**a**) sandy coastline; (**b**) silty coastline; (**c**) biological coastline; (**d**) artificial coastline; and (**e**) bedrock coastline.

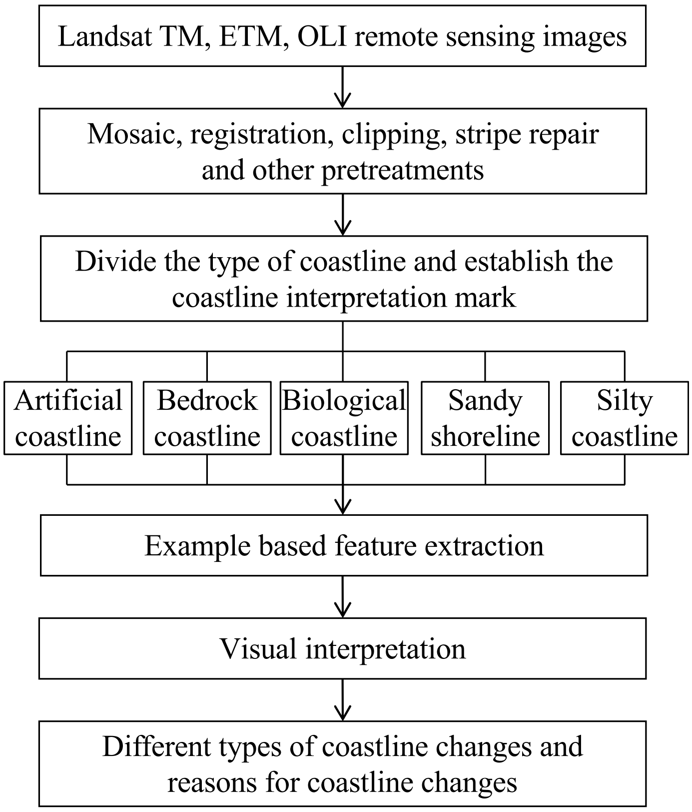

Figure 3. Technology route of coastline extraction.

According to the distinct features of the coastline illustrated by the Landsat images (e.g., the hue, texture, location and spatial form) the coastline interpretation markers were established and the principles of coastline extraction were determined [48]. Sandy coastlines are formed by sand and gravel accumulation at the seashore and usually present low water content and high brightness in remote sensing images. It is usually shown as a bright white "line" parallel to the seashore [11]. The inner boundary of the "line" is the location of the sandy coastline (Figure 2a).

Silty coastlines are mainly located in the nearshore with abundant sand and less erosion. In remote sensing images, these are gray or off-white. There are tidal gullies on the tidal flats, and the vegetation above the tidal flats generally grows luxuriantly and presents itself in reddish brown in remote sensing images. The location where the vegetation density changes significantly is the silty coastline [50] (Figure 2b). The biological coastline is formed by the growth and reproduction of plants and animals in the coastal waters. In this study, biological coastline refers to mangrove coastline, which is reddish brown in remote sensing images and distributed in patches in the bay area or river estuaries [51].

The inner boundary of the mangrove forest is where the biological coastline is located (Figure 2c). Artificial coastlines are formed by artificial activities in the process of development, with regular shapes and sharp edges. In remote sensing images, the spectral reflectance is high, and the texture is clear [11,52]. The outer boundary of the artificial buildings represents the position of the artificial coastline (Figure 2d). Last, the bedrock coastline is composed of rocks with zigzag shapes and evident contours. In remote sensing images, the spectral reflectance is low, and the predominant color is gray [52]. The sea-land boundary is the bedrock coastline (Figure 2e).

2.4. Coastline Length Calculation

In this study, the average change rate method was applied to calculate the change of coastline length of GHMGBA. This refers to the annual percentage change of coastline length over a certain period and is often used to express the change in intensity of the region, which can better illustrate its variations over time [53]. The average velocity is calculated as follows:

$$LCI_{mn} = (L_m - L_n)/L_n\ (m - n) \times 100 \tag{1}$$

where LCI_{mn} stands for the average rate of change of different types of coastlines in the $m - n$; L_m represents the length of the coastline in the year m; L_n represents the length of the coastline in the year n; and $L_m - L_n$ represents the change length in the determined period.

2.5. Accuracy Test

In this study, 50, 25, 5 and 15 points were randomly selected on the artificial coastline, bedrock, biological and sandy coastlines of 2018, respectively. An additional five points were randomly selected on the silty coastline of 2010. A total of 100 points were selected for testing. The distance between points and the coastline were obtained using the near dist analysis function in ArcGIS 10.3 software. The average value was 29.9 m, and the standard deviation was 18.2 m.

The average value of the artificial, bedrock, biological and sandy coastlines was about 30 m, and the standard deviation was less than 30 m. The error of the silty coastline was about two pixels. This may be related to the fact that the points were selected in 2000, a period far from 2017. The error in one pixel was in the normal range, satisfying the demands of this study [54]. Therefore, the coastline extraction methods used in this study are reliable and successfully meet the accuracy requirements for coastline changes.

3. Results

3.1. Changes in Coastline Length

Based on Landsat images, data from the coastlines of the GHMGBA in 1987, 1990, 2000, 2010 and 2018 were extracted (Figure 4), and their lengths were 1291, 1300, 1335, 1356 and 1411 km, respectively (Figure 5). The coastline showed an increasing trend as a whole, which included: (i) an increase of 10 km in the 1980s, with a variation rate of 0.3%, accounting for 7.9% of the total increase length; (ii) an increase of 35 km in the 1990s, with a variation rate of 0.3%, accounting for 29.2% of the total increase length; and (iii) an increase of 21 km in the 2000s, with a variation rate of 0.2%, accounting for 17.1% of the total increase length. In the 2010s, it increased by 55 km with a variation rate of 0.5%, accounting for 45.7% of the total increase length (Table 2). The major outcome of these procedures reveals that the coastline of the GHMGBA has increased by 120 km in the past four decades, with an overall variation rate of 0.3%.

3.2. Distribution and Types of Coastline

Information on the coastline of the GHMGBA in the 1980s, 1990s, 2000s and 2010s was obtained according to the five types of classification mentioned above (Figure 4). In the 1980s, the major changes happened in Huidong County of Huizhou City, Baoan District of Shenzhen City and Doumen District of Zhuhai City. In the 1990s, the major areas of change were Longgang District of Shenzhen City, Jinwan District of Zhuhai City and Duhu Town and Chixi Town of Taishan City of Jiangmen City. In the 2000s, Baoan District and Nanshan District of Shenzhen City as well as Jinwan District of Zhuhai City were the areas that changed the most. In the 2010s, the major areas of change were Huiyang District of Huizhou City, Futian District of Shenzhen City and Xiangzhou District of Zhuhai City.

Considering the same data, statistics were provided according to different types of coastlines (Figure 5). Among them, the artificial is the one that coastline has changed the most, with its length increasing from 406 km (31.5% of the total) in 1987 to 872 km (61.8% of the total) in 2018. In 1987, the artificial coastlines were mainly distributed in Nanshan District and Baòan District of Shenzhen City, Nansha District of Guangzhou City and Doumen District of Zhuhai City.

In 2018, they were mainly distributed in Nanshan District and Baòan District of Shenzhen City, Humen Town of Dongguan City, Nansha District of Guangzhou City, Doumen District and Xiangzhou District of Zhuhai City [55], Guanghai Town, Wencun Town and Haiyan Town of Taishan City, Jiangmen were distributed along the coast of the GHMGBA. In the last four decades, the artificial coastline increased by 465 km with an overall change rate of 3.7% (Table 2). It burgeoned in the 1980s and 1990s, but the pace slowed down in the 2000s and 2010s.

The bedrock shoreline decreased the most, with its length changing from 594 km in 1987 (46.0% of the total) to 407 km in 2018 (28.8% of the total). In 1987, it was mainly distributed in Huidong County and Huiyang District of Huizhou City, Longgang District of Shenzhen City, the eastern and southern coasts of Hong Kong, the southwest coast of Huangmao Sea and the west coast of Zhenhai Bay. In 2018, it was mainly distributed in Longgang District, Shenzhen City. In the past four decades, the bedrock coastline has decreased by 187 km, with an overall change rate of −1.0% (Table 2). It showed a trend of rapid decrease in the 1980s and 1990s, but the pace slowed down in the 2000s and 2010s.

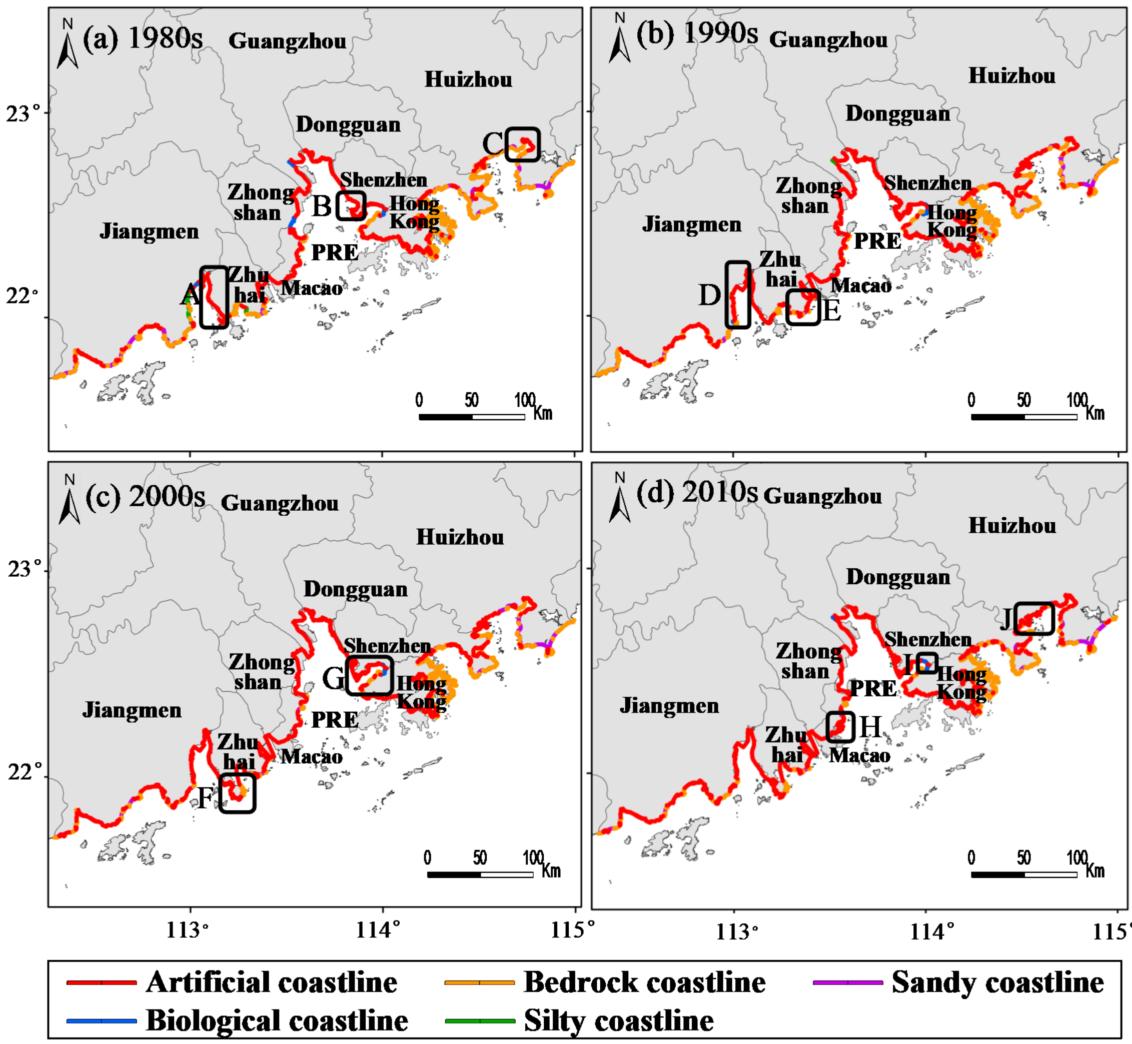

Figure 4. Distribution of different types of coastlines in the GHMGBA over four decades: (**a**) 1980s; (**b**) 1990s; (**c**) 2000s; and (**d**) 2010s. Box A: East coast of Huangmao Sea, Box B: Qianhai Bay, Box C: Fanhe Port in Huidong County, Box D: West coast of Huangmao Sea, Box E: Sanzao Island, Box F: Gaolan Island, Box G: Qianhai Bay, Houhai Bay and Shekou Peninsula, Box H: Jinwan District, Box I: Shenzhen Futian Mangrove Nature Reserve and Box J: Daya Bay Petrochemical Industrial Zone, located in Huiyang District.

The length of the biological shoreline decreased from 51 km in 1987 (4.6% of the total) to 16 km in 2018 (1.2% of the total). In 1987, the biological coastline was mainly distributed in Renshan Town, Huidong County of Huizhou City, Futian District of Shenzhen City, Nanlang Town of Zhongshan City and Xinhui District of Jiangmen City. In 2018, it was mainly distributed in Futian District of Shenzhen City. The biological shoreline has decreased by 42 km in the past forty years, with an overall change rate of −2.3% (Table 2). It showed a trend of rapid decrease in the 1980s and 1990s, slow decrease in the 2000s and increasing again in the 2010s.

The length of the sandy coastline decreased from 172 km in 1987 (13.3% of the total) to 116 km in 2018 (8.2% of the total). It was mainly distributed in Huidong County of Huizhou City, Longgang District of Shenzhen City, Haiyan Town and Beidou Town of Taishan City of Jiangmen City in 1987 and in Huidong County of Huizhou City in 2018. In the past forty years, the sandy coastline has decreased by a total of 56 km, with an overall change rate of −1.1% (Table 2) and a fluctuating trend of decrease.

The length of the silty coastline was about 60 km in 1987 (4.7% of the total), and all of it disappeared in the 2000s. In 1987, the silty coastline was mainly distributed in Bao'an District of Shenzhen City and Duhu Town and Chixi Town of Taishan City, Jiangmen City, with an overall change rate of −4.8% in the past four decades (Table 2).

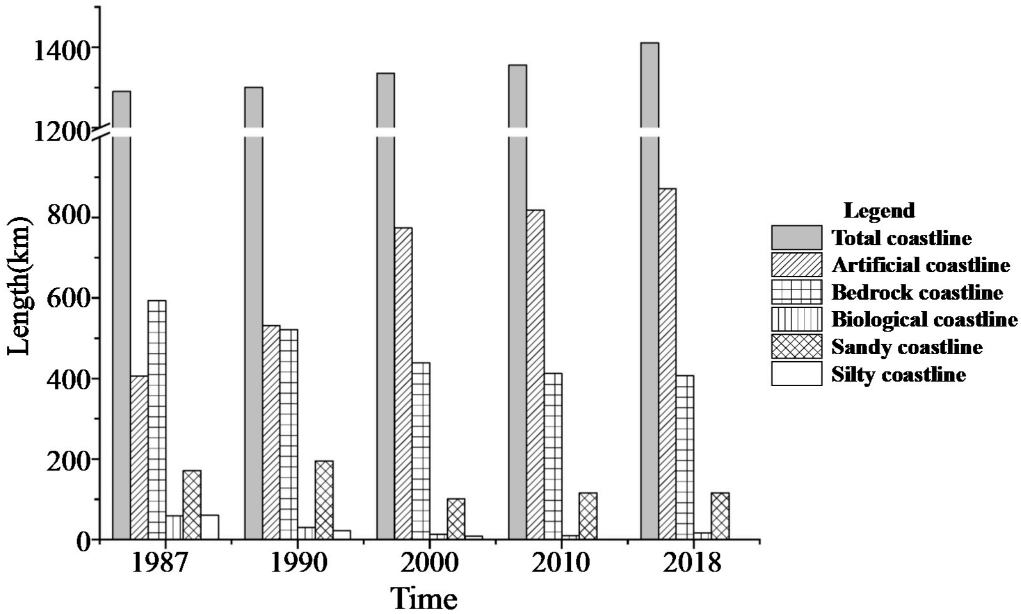

Figure 5. Coastline length in the GHMGBA at different times.

Table 2. Variation of coastline in the GHMGBA in different decades.

Period	Coastline Change (km)/Change Rate (%)						Proportion to Total Change (%)
	Artificial Coastline	Bedrock Coastline	Biological Coastline	Sandy Coastline	Silty Coastline	Total	
1980s	+125/+10.2	−72/−4.0	−29/−16.5	+24/+4.6	−37.84/−21.0	+10/0.3	7.9
1990s	+242/+4.6	−82/−1.6	−17/−5.6	−94/−4.8	−14/−6.4	+35/0.3	29.2
2000s	+44/+0.6	−27/−0.6	−3/−2.7	+15/+1.5	−8/−10.0	+21/0.2	17.1
2010s	+54/+0.8	−6/−0.2	+7/+8.9	0/0	0/0	+55/0.5	45.7
4 decades	+465/+3.7	−187/−1.0	−42/−2.3	−56/−1.1	−60/−4.8	+120/0.3	100

4. Discussion

4.1. Coastline Classification

In this study, we combined feature extraction and visual interpretation to extract coastline data, so we could make corrections based on the automatic extraction of an object-oriented coastline. Related studies classified coastlines into only four categories: bedrock, sandy, silty and artificial coastlines [56,57], because the term "biological coastline" generally refers to mangrove coastline, coral reef and reed coastlines, which are usually not distributed in some coastal areas. Here, biological coastline refers to mangrove coastline. Some studies provide a more detailed classification of coastlines, adding estuarine shorelines to the list [51], or classifying artificial coastlines considering other aspects, such as the existence of wharf coastlines, as well as agricultural, farming, salt land, construction and transportation dykes [51,58].

4.2. Major Change Areas of the GHMGBA Coastline

In the past four decades, the length of the Chinese mainland coastline has continued to expand and the intensity of change has gradually escalated. The coastline of the PRE presented significant changes. The growth of breeding dikes and port terminal coastline and farming reclamation as during 1980–2000 kept Guangdong among the top three coastal provinces in China. The area increased with new port infrastructures and became the largest in China [2]. Related studies have shown that the coastline of Guangdong Province advanced toward the ocean during 1980–2010 [59], a phenomenon that is consistent with the results of this study.

The coastline changes in the GHMGBA were mainly manifested by the transformation of natural to artificial coastlines. Major changes were found in Huidong County and Huiyang District of Huizhou City, Futian District, Baoan District and Nanshan District of Shenzhen City and Jinwan District of Zhuhai City. The areas where the transition from bedrock to artificial coastline was clear were Huidong County and Huiyang District of Huizhou City (Figure 4b). Fanhe Port in Huidong County (Box C in Figure 4a) is the mouth of many rivers, and the low flow rate of rivers leads to sedimentation. In addition, the port is located in the bay, where the tidal action is weak, and thus the erosion effect of the current on the beach is small [60]. Therefore, the fragmented land can easily be transformed into farming and industrial land. After 2000, the construction of Chinese ports and wharves entered a high-speed development stage [2]; therefore, the coastline near the Fanhe Port advanced to the ocean.

Located in Huiyang District of Huizhou City, the Daya Bay Petrochemical Industrial Zone (Box J in Figure 4d) is one of the key petrochemical industrial bases in Guangdong Province, and its construction changed the original coastline pattern. The rapid development of the petrochemical industry after 2000 expanded the demand for land, and the coastline of this specific zone extended to the ocean through land reclamation projects based on the original coastline. The convex embankment formed by the construction of the port terminals also increased the length of the artificial coastline [61]. As a result, it continues to increase until now.

The areas where the transformation of the silty coastline to the artificial coastline and the advancement of the original artificial coastline to the ocean is more evident are the east coast of Lingdingyang and the west coast of Huangmao Sea (Box D in Figure 4b). From 1990 to 2000, the average change rate in the length of the PRE coastline reached 15.5% [5], due to the expansion of urban land, the construction of transportation networks and the development of ports and terminals. Lingdingyang is the major inlet of the Pearl River, and its eastern coast has undergone tremendous changes in the past four decades. Among them, considerable changes affected the coastline of Shenzhen, especially regarding its spatial distribution [4].

Shenzhen Baòan International Airport was built based on land reclamation and was officially inaugurated in 1991. After 1993, the infrastructure of the airport was further improved, forming a relatively straight coastline that kept advancing towards the ocean [6].

Shenzhen's Qianhai Bay, Houhai Bay and Shekou Peninsula (Box G in Figure 4c) are the frontline of Shenzhen's economic development. In the 1980s, the Qianhai Bay and the Houhai Bay were dominated by sea-farming, and, after 2000, land reclamation episodes became frequent. The artificial farming area was filled in, the original aquaculture area was gradually transformed into towns, and the zigzag natural coastline was transformed into a straight artificial coastline.

The zigzag of the coastline decreased, and Qianhai Bay (Box B in Figure 4a) showed a trend of merging [61], while Houhai Bay gradually became smaller [62]. In the Shekou Peninsula, the continuous construction of infrastructure projects, such as ports, wharves and town facilities has straightened the original zigzag coastline [10,11,61]. In 1987, the silty coastline was widespread. In the 1980s, 1990s and 2000s, the area was dominated by the construction of pond farming constructions. The pond reclamation made the coastline advance to the ocean to form new artificial coastlines [61]. This is when the transformation of the silty coastline and the biological coastline to artificial coastlines became evident, and almost all of them were converted to artificial coastline in the 2010s.

The newly added artificial coastline performed significantly in the Jinwan District of Zhuhai City (Box H in Figure 4d). The Hong Kong-Zhuhai–Macao Bridge (HZMB) is a bridge-tunnel project connecting Hong Kong, Zhuhai and Macao in China, located in the Lingdingyang of PRE in Guangdong Province, China. The HZMB was constructed through a land reclamation project that took advantage of artificial islands [63]. Since the construction began in 2009, the original coastline shape has been continuously changed and the formation of two artificial islands has increased the length of the artificial coastline [11].

The Gaolan Island (Box F in Figure 4c) is located in the south of Jinwan District, Zhuhai City. In the 1980s, its northern side was dominated by sea farming. Since the embryonic stage of the project, in 2003, the land reclamation area has increased [10], resulting in the water area between islands and land being gradually filled. Once the gradual construction of the Zhuhai Port and the Gaolan Port was completed, and the islands were connected to the land around 2008 [10,61]. The Sanzao Island (Box E in Figure 4b) in the southeast of Huangmao Sea became a land-linked island in the 2010s, increasing the length of the coastline. After 2000, the construction of towns, the Jinwan International Airport, and new coastal transportation lines have also collaborated to increase the length of the artificial coastline [6,55].

The biological coastline (mangrove coastline) in the GHMGBA showed a trend of decreasing and then increasing. The decreasing trend in the biological coastline was a reality during the 1980s, 1990s and 2000s; however, in the 2010s, the scenario changed, and there was an increase of 7 km. The biological coastline was reduced by 42 km over the past four decades (Table 2). Guangdong Province has the largest mangrove distribution area in China [64], with about 120 km^2 (12,040 hectares), accounting for about 57.3% of the Chinese mangrove area [65].

The biological coastline retention rate in the GHMGBA declined and is currently at a low level (from 90% in 1973 to 34.5% in 2016) [66]. Early regional economic development and factories construction led to an increased demand for land and the destruction of the biological coastline [67]. In recent years, there has been an increasing awareness of the importance of mangrove conservation and restoration initiatives [68].

China has issued several related action plans for mangrove restoration [69] and related policies and regulations for marine development (http://www.forestry.gov.cn/, accessed on 3 August 2020), promoted the "Blue Bay" comprehensive improvement project, repaired damaged shorelines, increased the area of coastal wetlands and effectively controlled the scale of sequestration and reclamation [70]. The Shenzhen Futian Mangrove Nature Reserve (Box I in Figure 4d) is the second largest mangrove reserve in China. Its construction helps to purify water bodies, strengthen the shore protection, prevent wind and waves and promote siltation and beach preservation in the adjacent waters [11,55,62,67].

The silty coastline in the GHMGBA has been decreasing over the past four decades, with a total reduction of 60 km (Table 2). The major areas of change were two shores of the Huangmao Sea (Box A in Figure 4a and Box D in Figure 4b). The pond aquaculture and coastline development projects in the 1980s and 1990s transformed the silty coastline into artificial coastlines, resulting in its complete disappearance in the 2000s. Almost all the Huangmao Sea coastlines were transformed into an artificial coastline.

4.3. Major Reasons for Coastline Changes in the GHMGBA

The coastline changes in the GHMGBA in the past four decades can be explained by natural and human factors. Natural causes mainly include sediment deposition in estuaries, coastal erosion in areas with high wind and waves, river diversion and sea level rise due to global warming. However, these natural factors did not heavily influence the scenario. Human factors, on the other hand, are more directly related to these changes. These include land reclamation, urban construction, construction of ports and docks and national policies.

Major coastline variations were caused by human activities, even under different climatic conditions. In Mediterranean Climate, the coastline has been drastically modified by human interventions over the last two centuries [71]. In southeastern Spain, the coastline has changed due to human land reclamation to the sea in different periods (1956–1957 and 2014–2016) [72]. In the Athens Riviera, the coastline was enhanced by 40% from 1945 to 2021, while land reclaimed to the sea area now approached 2.7 km^2 because of human interventions. The growth of urban fronts in the coastal area resulted in this artificial increase of coastline length [73].

Reclamation is an effective method to solve the shortage of land resources in coastal areas. Relevant studies showed that, during 1980–2010, the land reclamation area in Liaoning Province was 358 km^2, mainly used for coastal industry, fishing ponds and town construction [74]. Guangdong province increased land reclamation by over 600 km^2, ranking the highest in China [60]. The PRE region is the most economically developed and fastest growing region in the area with a great demand for land for urban construction and port construction, and the scale of land reclamation is the largest in the province [75].

For small island countries, e.g., Indonesia, Malaysia and Singapore, land reclamation is an important way to increase the available land area, mainly used for urban construction and agricultural development [76]. In the 1980s, coastal towns in the GHMGBA developed planting and aquaculture through beach reclamation and pond culture at the estuary and bay area where tidal flats were deposited. In the 1990s, urban expansion covered the original agricultural areas, farming waters and polder boundaries advanced toward the sea, urban construction development sped up, and the construction of port wharfs increased [6]. Hence, coastal development changed the spatial pattern of the original coastline.

The development of coastlines brings great economic benefits but may also shine a light on environmental pollution and ecological problems [77]. Coastline changes may be related to global warming, rising sea levels and tropical cyclone activities [78]. In order to ease the conflict between human and nature, China promulgated Notice of the State Council on Several Issues Concerning Further Strengthening the Work of Marine Management (http://www.gov.cn/, accessed on 12 August 2020) and Regulations of Guangdong Province on the Administration of the Use of Sea Areas (http://www.gd.gov.cn/, accessed on 15 August 2020) to strictly approve marine development activities and control land reclamation and the mining of sea sand.

Management was, thus, gradually standardized. Ecosystem protection and restoration were strengthened, and the biodiversity level can, therefore, be maintained. From then on (2000–2018), the length change rate of the artificial coastline and bedrock coastline was relatively small, because national policies played a significant role. The length of the biological coastline increased, and the mangroves have slowly recovered, but small-scale land reclamation and water conservancy projects are still in progress. Therefore, it can be affirmed that the coastline changes in the GHMGBA are connected with human factors, such as beach reclamation, pond aquaculture, urban construction, land reclamation and national policies.

5. Conclusions

The GHMHBA coastline data of four decades (1980s, 1990s, 2000s and 2010s) was extracted using geographic information system (GIS) technology based on Landsat series multi-period remote sensing images. The total length of the coastline tended to increase, with the artificial coastline increasing the most, the bedrock coastline decreasing the most, and the silty coastline disappearing. These phenomena are connected with human activities such as land reclamation, town construction, port and wharf construction and national policies. The coastline as a whole showed a trend of advancing toward the ocean. Due to the strengthening of marine ecological and environmental protection in recent years, the coastline changes in the GHMGBA slowed down after 2000.

Author Contributions: R.H. and L.Y. designed the study. J.Y. and R.H. collected the data. R.H. analyzed the data. D.W. and P.C. helped with data collection and analysis. J.Y. and R.H. wrote the article. All authors have read and agreed to the published version of the manuscript.

Funding: This study was supported by the following funds: (1) R & D Projects in Key Areas of Guangdong Province, China (2020B1111030002), (2) National Key R & D Program of China (2018YFD0900901), (3) Natural Science Foundation of Guangdong Province, China (2018A030313120), (4) Central Public-Interest Scientific Institution Basal Research Fund, CAFS, China (2018HY-ZD0104).

Institutional Review Board Statement: Not applicable.

Informed Consent Statement: Not applicable.

Data Availability Statement: Data available on request due to restrictions, e.g., privacy or ethical. The data presented in this study are available on request from the corresponding author. The data are not publicly available due to privacy policy.

Conflicts of Interest: The authors declare no conflict of interest.

References

1. Fan, Q.; Liang, L.; Liang, F.; Sun, X. Research Progress on Coastline Change in China. *J. Coast. Res.* **2020**, *99*, 289–295. [CrossRef]
2. Xu, N. Research on Spatial and Temporal Variation of China mainland Coastline and Coastal Engineering. Ph.D. Thesis, Yantai Insititute of Coastal Zone Research, Chinese Academy of Sciences, Yantai, China, May 2016.
3. Jia, M.; Liu, D.; Wang, Z.; Tang, X.; Dong, Z. Coastline Changes in Hangzhou Bay Based on Object-oriented Method Using Multi-source Remote Sensing Data. *J. Geo-Inf. Sci.* **2013**, *15*. [CrossRef]
4. Xia, H.; Long, Y.; Liu, C.; Liu, X. Spatial pattern change of the coastline development and utilization in the Pearl River delta from 1973 to 2018. *J. Mar. Sci.* **2020**, *38*, 26–37.
5. Liu, X.; Deng, R.; Xu, J.; Gong, Q. Spatiotemporal evolution characteristics of coastlines and driving force analysis of the Pearl River Estuary in the past 40 years. *J. Geo-Inf. Sci.* **2017**, *19*, 1336–1345.
6. Wang, J.; Wu, Z.; Li, S.; Wang, S.; Zhang, X.; Gao, Q. Coastline and land use change detection and analysis with remote sensing in the Pearl River estuary gulf. *Sci. Geogr. Sin.* **2016**, *36*, 1903–1911.
7. Quang, D.N.; Ngan, V.H.; Tam, H.S.; Viet, N.T.; Tinh, N.X.; Tanaka, H. Long-Term Shoreline Evolution Using DSAS Technique: A Case Study of Quang Nam Province, Vietnam. *J. Mar. Sci. Eng.* **2021**, *9*, 1124. [CrossRef]
8. Xia, Z.; Jia, P.; Lei, Y.; Chen, Y. Dynamics of coastal land use patterns of inner Lingdingyang Bay in the Zhujiang River estuary. *Chinese Geogr. Sci.* **2007**, *17*, 222–228. [CrossRef]
9. Li, X.; Damen, M.C.J. Coastline change detection with satellite remote sensing for environmental management of the Pearl River Estuary, China. *J. Marine Syst.* **2010**, *82*, 54–61. [CrossRef]
10. Zhang, Y.; Li, X.; Ma, Y.; Bao, Y. Analyzing shoreline changes of the Pearl River Estuary based on remote sensing. *Hydrogr. Surv. Charting* **2014**, *34*, 52–55.
11. Zhang, Y.; Zhang, Q.; Hu, Y. Remote sensing monitoring and dynamic analysis of the Pearl River Estuary coastline during 2010–2017. *Mar. Sci. Bull.* **2019**, *38*, 217–224.
12. Zhang, Y. Analyzing Shoreline Changes of the Pearl River Estuary Based on Remote Sensing in Recent Forty Years. Master's Thesis, Inner Mongolia Normal University, Huhehaote, China, 2014.
13. Ali, K.; Sarah, M.; Brian, G.; Carl, A.; Yasir, M. Geoinformatics vulnerability predictions of coastal ecosystems to sea-level rise in southeastern Australia. *Geomat. Nat. Hazards Risk* **2018**, *9*, 645–661.
14. Yu, J.; Chen, P.; Jia, X.; Tang, Z.; Qin, C. Research progress on coastline extraction based on remote sensing and GIS technique. *J. Anhui Agri. Sci.* **2012**, *40*, 15989–15991.
15. Yu, J.; Hu, Q.; Li, C.; Zhang, P.; Mao, J. Relationship between the symplectoteuthis oualaniensis resource and environmental factors in the Xisha-Zhongsha waters in spring. *Acta Oceanol. Sin.* **2017**, *39*, 62–73.

16. Rodríguez-Santalla, I.; Navarro, N. Main Threats in Mediterranean Coastal Wetlands. The Ebro Delta Case. *J. Mar. Sci. Eng.* **2021**, *9*, 1190. [CrossRef]
17. Zhu, H.; Xing, B.; Ni, S.; Wei, P. Study on the coastline change of jiaozhou bay based on high resolution remote sensing image. *ISPRS Int. Arch. Photogramm. Remote Sens. Spat. Inf. Sci.* **2018**, *XLII-3*, 2591–2597. [CrossRef]
18. Li, J.; Zhang, Y. The Change and Analysis of Coastline Based on Remote Sensing Measurement. In Proceedings of the 2011 IEEE International Conference on Spatial Data Mining and Geographical Knowledge Services (ICSDM 2011), Fuzhou, China, 29 June 2011.
19. Huang, J.; Zhao, G. Spatiotemporal change of sediment siltation and erosion dynamics and its influences on water and sediment budgets of the yellow river mouth in the past 20 years based on remote sensing and GIS date. *Mar. Geol. Front.* **2021**, *37*, 16–21.
20. Sun, Y.; Yang, F.; Tian, S.; Li, X.; Tu, Z. The design and application of monitoring system for reclamation projects based on multi-source remote sensing images. *Ocean. Dev. Manag.* **2020**, *37*, 84–88.
21. Sun, S. Reclamation Information Extraction Using Decision Tree Method in Jinzhou Bay Area. Master's Thesis, Liaoning Normal University, Dalian, China, May 2015.
22. Wang, Z.; Gao, Z. Analysis on spatiotemporal characteristics and causes of tidal flat wetland in Jiaozhou Bay from 1987 to 2017 based on land use change. *Res. Soil Water Conserv.* **2020**, *27*, 196–201.
23. Kang, Y.; Lv, W.; He, J.; Ding, X. Remote Sensing of Time-Varying Tidal Flat Topography, Jiangsu Coast, China, Based on the Waterline Method and an Artificial Neural Network Model. *Appl. Sci.* **2020**, *10*, 3645. [CrossRef]
24. Zhang, Y.; Gao, Z.; Liu, X.; Xu, N.; Liu, C. Study on the extraction method of tidal flat area in northern Jiangsu Province based on remote sensing waterlines. *Opt. Eng. Appl.* **2016**, *9975*, 99750M. [CrossRef]
25. Ding, X.; Shan, X.; Chen, Y.; Jin, X.; Muhammed, F.R. Dynamics of shoreline and land reclamation from 1985 to 2015 in the Bohai Sea, China. *J. Geogr. Sci.* **2019**, *29*, 2031–2046. [CrossRef]
26. Huang, S.; Wei, C. Spatial-temporal changes in aquaculture ponds in coastal cities of Guangdong Province: An empirical study based on sentinel-1 data during 2015–2019. *Trop. Geogr.* **2021**, *41*, 622–634.
27. Wang, Z.; Gao, Z.; Shang, W.; Jiang, X. Land use change and its influence on coastline change along Laizhou Bay during 1987–2017. *Bull. Soil Water Conserv.* **2021**, *41*, 309–316+336.
28. Song, C.; Liu, G. Dynamic Analysis of the Vegetation Pattern of the Yellow River Delta National Nature Reserve Basedon Remote Sensing. In Proceedings of the 3rd International Yellow River, Dongying, China, 16 October 2007.
29. Qiao, X.; Wang, Q.; Zhan, C.; Wang, H.; Du, G.; Li, X. Progress of research in coastline Extraction based on RS Technique. *J. Ludong Univ.* **2016**, *2*, 158–161.
30. Yuan, X.; Wang, P.; Zhang, Y.; Ren, L.; Zhai, L. Research on edge detection and object-oriented for automatic extraction of coastline. *Beijing Surv. Mapp.* **2019**, *33*, 148–152.
31. Yan, H.; Li, B.; Chen, M. Progress of researches in coastline extraction based on RS technique. *Areal Res. Dev.* **2009**, *28*, 101–105.
32. Ju, C. Research on Automatic Extraction of Coastline from GF1 Remote Sensing Images Based on Object-oriented. Master's Thesis, Liaoning Technical University, Fuxin, China, June 2017.
33. Zhang, Y.; Guo., Y.; Zhang, F. Research on coastline extraction based on remote sensing technology. *Sci. Technol. Innov.* **2013**, *33*, 44, 139.
34. Wang, F.; Liu, S.; Lu, W.; Du, Q.; Jiang, W.; Liu, J. Island instantaneous coastline extraction based on the characteristics of regional statistics of multispectral remote sensing image. *Mar. Sci. Bull.* **2014**, *16*, 25–37.
35. Zhang, J.; Lai, Z.; Sun, J. Coastline extraction of remote sensing image by combining Otsu, regional growth method with morphology. *Bull. Surv. Mapp.* **2020**, *10*, 89–92.
36. Zhai, H. Research on Surface Object Extraction from Remote Sensing Image based on Mathematical Morphology. Master's Thesis, Information Engineering University, Zhengzhou, China, April 2005.
37. Liang, L.; Liu, Q.; Liu, G.; Li, X.; Huang, C. Review of coastline extraction methods based on remote sensing images. *J. Geo-Inf. Sci.* **2018**, *20*, 1745–1755.
38. Zhong, S.; Wang, Q.; Zhan, C.; Li, X.; Wang, X. Changes land-use of the supratidal zone of typical sandy coast along eastern Laizhou Bay in recent 50 years. *Oceanol. Limnol. Sin.* **2015**, *46*, 410–419.
39. Li, Z. Development Research on Marine-inland Economic Integration in Guangdong-Hong Kang-Macau Greater Bay Area. Ph.D. Thesis, Liaoning University, Liaoning, China, December 2018.
40. Ma, C.; Lin, X. A new trend in the integrated development of the Guangdong-Hong Kong-Macao Greater Bay Area. *Co-Oper. Econ. Sci.* **2020**, *11*, 43–45.
41. Xiao, L. Brief analysis on the significance and role of the construction of Guangdong-Hong Kong-Macao Greater Bay Area in the new round of opening-up in China. *Mark. Mod.* **2019**, *21*, 112–114.
42. Zhen, Y. The importance and path of strengthening and improving the "Belt and Road" publishing cooperation in the new period. *Publ. J.* **2021**, *29*, 5–13.
43. Hu, X.; Wang, Y. Coastline Fractal Dimension of Mainland, Island, and Estuaries Using Multi-temporal Landsat Remote Sensing Data from 1978 to 2018: A Case Study of the Pearl River Estuary Area. *Remote Sens.* **2020**, *12*, 2482. [CrossRef]
44. Sun, P.; Gong, C.; Hu, Y.; Zhang, W.; Song, W. Extraction and change detection of Shanghai continental coastline using RS imagery in recent 30 years. *Infrared* **2017**, *38*, 20–27.

45. Gao, X.; Jiang, Q.; Li, Y.; Xi, J. Researching for Coastline Extraction Method Based on Object-oriented in North Shore of Hormuz Strait. In Proceedings of the 15th National Security Geophysics Symposium, Zhangye, China, 13 August 2019.
46. Sun, L. Coastline Changes Monitoring with Remote Sensing of the Zhejiang Province and Research on Coastal Vnlnerability Assessment. Master's Thesis, The First Institute of Oceanography, Qingdao, China, June 2013.
47. Special Office 908 of State Oceanic Administration. *Special Technical Regulations for Offshore Ocean Comprehensive Survey and Evaluation in China*; China Ocean Press: Beijing, China, 2006.
48. Kang, B. Spatial-temporal Changes of the Coastline in Five South Island of Long Island in Recent Three Decades on RS and GIS. Master's Thesis, Shanghai Ocean University, Shanghai, China, 19 May 2017.
49. Lin, N.; Huang, N.; Xu, W. Research on the model of coastline demarcation and management. *Mar. Sci. Bull.* **2009**, *11*, 82–89.
50. Yin, F.; Tian, L.; Wang, T.; Lv, L. Study on methods of Coastline remote sensing interpretation and extraction. *Geospat. Inform.* **2018**, *16*, 64–66, 83, 88.
51. Bao, M. Monitoring and Analyzing Hainan Island Coastline Dynamic Using Remote Sensing Imagery in Recent 40 Years. Master's Thesis, Inner Mongolia Normal University, Huhehaote, China, 26 May 2014.
52. Tang, J.; Xue, Q.; Li, G.; Zhu, B. Research on the temporal and spatial evolution of the Quanzhou Bay coastline. *South China J. Seismol.* **2020**, *40*, 137–147.
53. Zhu, G.; Su, F.; Zhang, J. Analysis on spatial-temporal changes of the coastline in the countries around the South China Sea in recent two decades. *Mar. Sci. Bull.* **2015**, *34*, 481–490.
54. Hu, Y. Shoreline Remote Sensing Extraction of the Taiwan Island and Evolution Characteristics Analysis in Recent 35 Years. Master's Thesis, Inner Mongolia Normal University, Huhehaote, China, 4 June 2016.
55. Lin, J.; Tang, D.; Gao, Y.; Li, X. Remote sensing of the classification, development and utilization of coastline in Zhuhai City. *Ocean. Dev. Manag.* **2019**, *36*, 69–73+93.
56. Ma, X. The Means of Withdrawing Coastline by Remote Sensing. Master's Thesis, Dalian Maritime University, Dalian, China, March 2007.
57. Xie, X. Study on extraction method of the coast-line based on the remote sensing image. *Geol. Fujian* **2012**, *31*, 60–66.
58. Gao, Y.; Su, F.; Zhou, C.; Yang, X.; Sun, X.; Zhang, D. Scale effects of China mainland coastline based on fractal theory. *Acta Geogr. Sin.* **2011**, *66*, 331–339.
59. Gao, Z.; Liu, X.; Ning, J.; Lu, Q. Analysis on changes in coastline and reclamation area and its causes based on 30-year satellite data in China. *Trans. China Soc. Agric. Eng.* **2014**, *30*, 140–147.
60. Yang, W.; Huang, D.; Chen, J.; Chen, X.; Wang, Y. Spatio-temporal distribution and eutrophication assessment of nutrients in Daya Bay during 2009–2015. *South China Fish. Sci.* **2020**, *16*, 54–61.
61. Zhu, J.; Wang, G.; Zhang, J.; Huang, T. Remote sensing investigation and recent evolution analysis of Pearl River delta coastline. *Remote. Sens. Land Resour.* **2013**, *25*, 130–137.
62. Yue, W.; Yan, B.; Zhang, T. Analysis of change of coastline in the Pearl River estuary based on the fractal theory. *Ocean. Dev. Manag.* **2020**, *37*, 38–41.
63. Zhu, Y.; Lin, M.; Meng, F.; Liu, X.; Lin, W. The Hong Kong-Zhuhai-Macao Bridge. *Engineering* **2019**, *5*, 10–14. [CrossRef]
64. Jiang, R.; Wu, Y.; Chen, P. Study on distribution of sediment carbon and nitrogen in mangrove wetland of Qi'ao Island, Pearl River Estuary. *South China Fish. Sci.* **2021**, *17*, 1–9.
65. Yang, J.; Hu, Y.; Luo, Y.; Xue, C. Study on the distribution and dynamic change of mangrove in Guangdong. *For. Environ. Sci.* **2018**, *34*, 24–27.
66. Huang, B.; Lu, X.; Chen, T.; Liu, W.; Lu, C. Study on the countermeasures of promoting the high-quality development of economy and high level protection of ecological environment in Guangdong-Hong Kong-Macao Greater Bay Area. *Environ. Sustain. Dev.* **2020**, *45*, 86–89.
67. Zhao, M.; Kou, J.; Yang, J.; Zhao, W. Study on the ecological security and protection measures of the coastal zone in Guang-dong-Hong Kong-Macao Greater Bay Area. *Environ. Prot.* **2019**, *47*, 29–34.
68. Tin, C.H.; Ni, K.N.; Tuan, V.L.; Isuzu, S.; Robert, C. Spatial and temporal variability of mangrove ecosystems in the Cu Lao Cham–Hoi an Biosphere Reserve, Vietnam. *Reg. Stud. Mar. Sci.* **2019**, *27*, 100550. [CrossRef]
69. Chao, B.; Wang, Y.; Yu, W.; Ma, Z.; Chen, G.; Chen, B.; Hu, W. Predicting mangrove forest dynamics driven by coastal land uses in Guangdong Province. *China Environ. Sci.* **2021**, *2021*, 1–12.
70. Zhao, W.; Yang, J.; Zhao, X.; Kou, J. Study on marine ecological environment protection and supervision strategy in Guang-dong-Hong Kong-Macao Greater Bay Area. *Environ. Prot.* **2019**, *47*, 21–23.
71. Anthony, E.J. The Human inflfluence on the Mediterranean coast over the last 200 years: A brief appraisal from a geomorphological perspective. *Geomorphol. Relief Process. Environ.* **2014**, *20*, 219–226. [CrossRef]
72. Llorens, P.M.; Pedreño, J.N.; Mingorance, J.M.S. Coastal line changes in Mediterranean cities: Man or nature? *WTBE* **2018**, *179*, 103–112.
73. Skilodimou, H.; Antoniou, V.; Bathrellos, G.; Tsami, E. Mapping of Coastline Changes in Athens Riviera over the Past 76 Year's Measurements. *Water* **2021**, *13*, 2135. [CrossRef]
74. Suo, A.; Zhang, M. Sea Areas Reclamation and Coastline Change Monitoring by Remote Sensing in Coastal Zone of Liaoning in China. *J. Coast. Res.* **2015**, *73*, 725–729. [CrossRef]

75. Ruan, B.; Zeng, L.; Qiu, Y. Evolution analysis of reclamation in Guangdong Province during 2006–2015. *Ocean. Dev. Manag.* **2020**, *37*, 9–12.
76. Yan, J.; Su, F.; Wang, M. The development processes and regional differentiation of both banks of the Strait of Malacca during 1980–2010. *Ocean Coast. Manag.* **2017**, *139*, 141–152. [CrossRef]
77. Yang, K.; Xu, N.; Long, Y.; Zhang, S.; Zhang, Y. The approach of safeguarding comprehensive environmental governance on green development in Guangdong-Hong Kong-Macao Greater Bay Area. *Environ. Prot.* **2019**, *47*, 54–55.
78. Tebaldi, C.; Ranasinghe, R.; Vousdoukas, M.; Rasmussen, D.J.; Vega-Westhoff, B.; Kirezci, E.; Kopp, R.E.; Sriver, R.; Mentaschi, L. Extreme sea levels at different global warming levels. *Nat. Clim. Chang.* **2021**, *11*, 746–751. [CrossRef]